

PAPER: Interdisciplinary statistical mechanics

# Evacuation through area with obstacle that can be stepped over: experimental study

Zhongjun Ding, Zhiwei Shen, Ning Guo<sup>1</sup>, Kongjin Zhu and Jiancheng Long

School of Automotive and Transportation Engineering, Hefei University of Technology, Hefei 230009, People's Republic of China

E-mail: [guoning\\_945@126.com](mailto:guoning_945@126.com)

Received 7 June 2019

Accepted for publication 9 December 2019

Published 20 February 2020



Online at [stacks.iop.org/JSTAT/2020/023404](https://stacks.iop.org/JSTAT/2020/023404)  
<https://doi.org/10.1088/1742-5468/ab6a01>

**Abstract.** This paper reports on a series of evacuation experiments exploring the impact of different obstacles on crowd dynamics. The experiments include three scenarios: evacuation without any obstacle (NO), evacuation with a bar-type obstacle in which the participants can choose to pass by or step over (CO), and evacuation with a bar-type obstacle in which the participants can only pass by (PO). The height of the obstacle and the distance between the obstacle and the exit in the CO cases are also taken into account. The evacuation times in the CO cases are basically longer than those in the PO cases. But a low CO obstacle very close to the exit can enhance the evacuation efficiency, compared to that of a PO obstacle. As the height of the CO obstacle increases, the pedestrian cluster around the exit separates into two clusters around the obstacle corners. In addition, the longer the distance between the CO obstacle and the exit, the fewer pedestrians prefer to step over the obstacle.

**Keywords:** nonlinear dynamics, traffic and crowd dynamics

<sup>1</sup> Author to whom any correspondence should be addressed.

## Contents

<b>1. Introduction</b>	<b>2</b>
<b>2. Experiment setup</b>	<b>4</b>
<b>3. Experimental results</b>	<b>6</b>
3.1. Evacuation time.....	6
3.2. Density evolution.....	14
3.3. Evacuation time gap.....	15
3.4. Step over or bypass the obstacle .....	16
<b>4. Conclusions</b>	<b>17</b>
<b>Acknowledgments</b> .....	<b>17</b>
<b>References</b>	<b>17</b>

## 1. Introduction

Research in the field of pedestrian traffic started in the early twentieth century [1, 2]. Until now, it has been sociologists and psychologists who have studied emergency crowd dynamics [3]. In recent years, due to increasing large-scale activities, many people have been involved in emergency incidents. In emergency situations, it is crucial to evacuate pedestrians in public infrastructure quickly and efficiently, and pedestrians may lose their survival chances with even a slight delay [4]. Hence, plenty of in-depth studies have been conducted of pedestrian dynamics in evacuations. Many evacuation experiments have been carried out, including animal experiments and human experiments [5–9]. As it is unethical to conduct a human experiment in a real hazardous condition, many simulation models have been proposed, such as the social force model (SFM) [4], the lattice gas model [10], and so on. Many evacuation characteristics have been discovered, such as the ‘faster is slower’ effect, arch formation phenomena, herding behavior. Also, many factors will affect the evacuation process.

Multivelocity is a crucial factor in crowd evacuation. In real emergency conditions, the differences in physiological functions, such as age, gender, walking abilities, may cause different evacuation speeds and crowd dynamics. Shahhoseini and Sarvi set a crowd merging experiment [11], showing that clogging arises more easily when pedestrians are told to evacuate as quickly as possible. Fu *et al* [12] built a floor field cellular automaton (CA) to simulate evacuation considering different pedestrian walking abilities. It is recognized that evacuees with higher velocities make the system jam more easily. Zhou *et al* [13] used a CA model to simulate pedestrian flow with multivelocities. It is found that the slowest pedestrian has a great impact on the average crowd velocity.

Another key element for crowd evacuation is the evacuation environment. After an earthquake or fire disaster, power cuts or smoke may limit the visual area of pedestrians.

Isobe *et al* [14] and Nagai *et al* [15] studied the evacuation process without visibility by means of experiments and simulations. Participants move slowly towards walls and then walk along next to them. Guo *et al* [16] carried out an evacuation experiment under conditions of good and zero visibility to study the behavior of route choice, and then a microscopic pedestrian model was developed to reproduce the experiment results. It is found that pedestrians generally prefer to touch the reference objects and then move along them. Wang *et al* [17] also investigated the evacuation efficiency under limited visibility and different evacuation strategies. The modified SFM simulation shows that in low densities it is more efficient for pedestrians to move along the walls when evacuating without visibility.

Architectural layout is an important factor in room evacuation, especially the distribution of obstacles around the exit. Helbing *et al* [5] organized an experiment to study the impact of obstacles on crowd evacuation. Pedestrians have to pass by the obstacle to escape from the room, helping to weaken the arching effect near the exit. The results show that the presence of obstacles increases the outflow by about 30%. Yanagisawa *et al* [18] conducted an experiment at the NHK TV studio in Japan to study the effect of an obstacle in front of the exit. It is found that compared with normal evacuation without obstacles near the exit, the setting of obstacles increases the outflow by about 7%. Jiang *et al* [7] designed multi-obstacle scenarios, observing that setting two obstacles near the exit is better than one or no obstacles near the exit. Although many experimental results show that an obstacle has some beneficial effect on the outflow of pedestrians near an exit, there is controversy about whether obstacles can play a good role in real evacuations. Liu *et al* [19] carried out a series of experiments to examine the influence of different exit designs on evacuation efficiency. It turned out that the obstacle in their experiments decreased evacuation efficiency. Shi *et al* [20] conducted a series of controlled experiments to investigate the influence of different building layouts on pedestrian evacuation. It is shown that whether obstacles can enhance the evacuation efficiency at the exit or not mainly depends on the size and location of the obstacles. Garcimartín *et al* [21] conducted three series of evacuation drills to figure out whether the existence of obstacles will improve the evacuation efficiency. Results show that the obstacle in their experiments did not improve the efficiency of evacuation, and the role of obstacles in pedestrian evacuation should be redefined. Shiwakoti *et al* [22] presents a critical review of the performance of obstacles near an exit.

As mentioned above, the impact of obstacles on crowd evacuation has been studied widely. However, we found that obstacles in previous studies were usually an extra infrastructure set near the exit and not allowed to be stridden over. In the real world, there are many small objects, which can become obstacles if they fall down to the ground in the evacuation, such as chairs, rocks and even pedestrians who have fallen. Lu *et al* [23] proposed a debris distribution model to show the possible distribution area of fallen objects. If the objects are put near the door of the room in the decoration design, they may become small obstacles after the earthquake or other disaster. Delcea *et al* [24] investigated the behavior choice of pedestrians when facing a fallen-down chair in the aisle in a classroom evacuation experiment. It is found that jumping over the chair costs less time than bypassing. In addition, dwarf obstacles still exist in real life, such as a gate machine in a subway station, a doorsill in ancient Chinese architecture and so on. Though these facilities are different from the obstacles that we are

discussing here, when an emergency occurs, these objects may act as a kind of special dwarf obstacle, affecting evacuation. For example, in an earthquake or fire disaster, the electric power may be cut, and pedestrians would have to climb over the enclosure of the gate machine to evacuate. A doorsill is a common design in ancient Chinese architecture, i.e. a small block stone or plank at the exit. In scenic spots and historical sites, there are many travelers, so it is necessary to study the effect of doorsills, i.e. a small obstacle, on evacuation. However, few studies investigate the effect of a small obstacle on evacuation dynamics and efficiency. In this work, we carry out an evacuation experiment with a bar-type obstacle; pedestrians can choose to go over it or bypass it. Generally speaking, the obstacle will increase the evacuation time. As the height of the obstacle increases, more pedestrians prefer to pass by the obstacle.

The remainder of this paper is outlined as follows. In section 2 the experimental setup is described. In section 3 the experimental results are presented and analyzed. In the last section, some conclusions are drawn from the present study.

## 2. Experiment setup

The experiments were performed on 13 October 2018 in Hefei University of Technology, and approved by the security department of Hefei University of Technology. We invited the participants via social network, and 52 participants (all college students, 11 females, 41 males) accepted the invitations. No participant quitted the experimental process. After the experiments, each participant would be paid 50 RMB. Experiments were conducted in an artificial square room with only one exit located in the middle of one wall (figure 1(a)). Three sets of experiments were conducted. The first is evacuation without any obstacle (NO). The second is evacuation with an obstacle, in which the participants can choose to pass by or step over the obstacle (CO). The third is evacuation with an obstacle, in which the participants can only pass by the obstacle (PO), i.e. the traditional obstacle as in previous studies [25]. The width of the virtual room is set as 7 m, and the width of the exit is 0.8 m. At the boundary of the virtual room, some chairs were tied by tape to represent walls, and two tables form the exit, see figures 1(b)–(d). A brick is used as the bar-type obstacle, which is 1.8 m in length, 0.3 m in width, and 0.15 m in height. The obstacle height can be tuned by palletizing the brick.

The obstacle was set in the middle line of the room, in both the CO and PO experiments. In the CO experiments, there were two design factors: the height  $h$  of the obstacle, the distance  $d$  between the obstacle and the exit. In the PO experiments, only the distance between the obstacle and the exit was taken into consideration. Each experiment with the same setup was repeated three times in a row. Details of the experimental setups and chronological order are given in table 1.

All 52 participants took part in every run of all the experiments. The participants knew exactly where the exit was, and were asked to escape from the room normally after the start command. Slight pushing and squeezing was allowed, but aggressive pushing and squeezing were strictly prohibited for safety reasons. Thus our experiment did not reflect the panic of a genuine emergency. Participants were told that if the command ‘stop’ was heard in the experimental process, they must stop moving

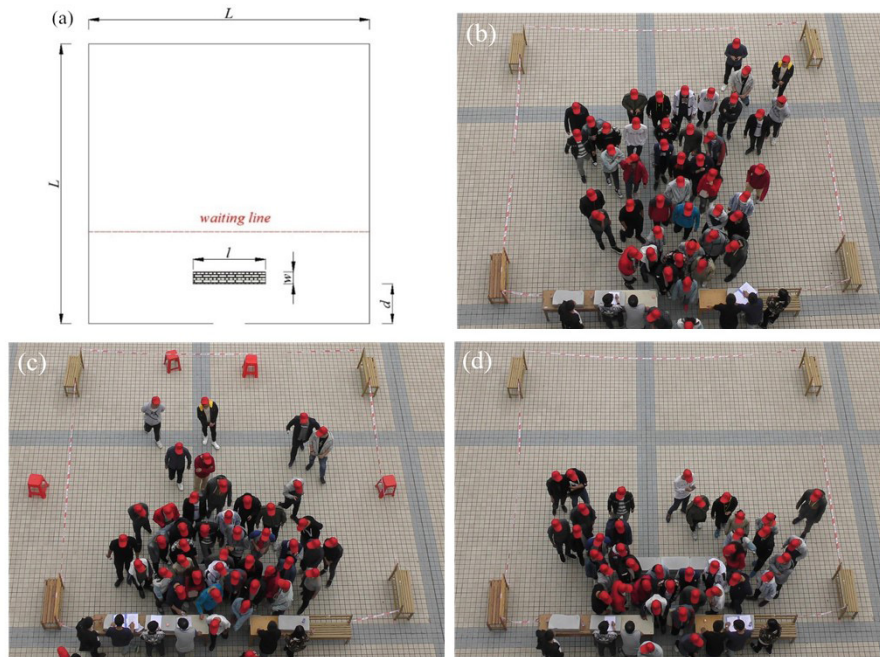


**Figure 1.** (a) Schematic diagram of experimental layout; (b)–(d) snapshots of experiments. (b) NO; (c) CO,  $h = 30$  cm,  $d = 100$  cm; (d) PO,  $d = 100$  cm.

**Table 1.** Experimental setup.

Sequence number	Obstacle type	Obstacle height (cm)	Distance between obstacle and exit (cm)
1–3	NO	/	/
4–6	PO	/	100
7–9	CO	60	100
10–12	CO	45	100
13–15	CO	30	100
16–18	CO	30	50
19–21	CO	45	50
22–24	CO	60	50
25–27	PO	/	50
28–30	CO	30	75
31–33	CO	45	75
34–36	CO	60	75
37–39	PO	/	75

immediately for safety reasons. Before each experimental run, the individuals stood randomly behind the waiting line, 2 m away from the wall where the exit was located.

To keep the tables stable, heavy bricks were put on the tables. Also, some experimental controllers stood near the tables and held the tables still with their hands. Because aggressive pushing and squeezing were forbidden, no severe contact between walkers and tables occurred. After each run of the experiment, we measured the exit width, and it was always 0.8 m. Before the experiment, participants were told that it was one virtual room, and the bottleneck could be imagined to be one door. So in the experiment, participants moved as if they were passing through a real door. No obvious over-leaning or side-moving behavior occurred.

The whole process of the experiment was recorded by high-definition video camera (Panasonic HC-VX980) at 25 frames per second, and the evacuation times were recorded manually according to the video record frame by frame. We could also collect the coordinate of every participant manually according to the square tiles on the floor.

### 3. Experimental results

#### 3.1. Evacuation time

The evacuation time of each pedestrian is given in figure 2. It is found that the evacuation times show a linear tendency in all experiments. A similar phenomenon has also been given in [8]. To analyze the degree of linearization quantitatively, the RMSE between the fitting line and the experiment results is used,

$$\text{RMSE}(i) = \sqrt{\frac{1}{m} \sum_{j=1}^m [g_i(j) - y_j]^2}. \quad (1)$$

Here  $m$  is the total number of pedestrians.  $y_j$  is the evacuation time of  $j$ th pedestrian escaping from the room in the experiment.  $g_i$  is the function of the fitting line. Here we assume that the fitting line is a line crossing the first experimental point and the  $i$ th experimental point. In figure 2, one line of  $g_i$  ( $i = 40$ ) is shown. Then RMSE of each  $g_i$  in each experiment can be obtained. The RMSE represents the linearity degree. As shown in previous studies [8, 26, 27], the evacuation time shows linear tendency. It is plausible that the smaller the RMSE between the fitting line and experiment results, the higher the linearity degree. Generally speaking (figure 3), the RMSE firstly reduces in pace with the increase of  $i$ . The reason is that if the span between the first point and point  $i$  is small, the small fluctuation will be amplified, leading to a big difference between the fitting line and the evacuation time of the last pedestrians. Until around  $i = 40$ , RMSE reaches the minimum. Then, RMSE increases again. It is because of this that our experiment is similar to an evacuation drill, and the last participants do not regard the experiment as a real evacuation. They are lazier than other participants and care less about the evacuation time. They keep a longer headway with the front participants. Therefore, the linearization degree of evacuation time is weakened by the last participants. To study the evacuation process better and eliminate the effect of the last inactive participants, we use the minimum of the RMSE to show the highest linearity, and only investigate the evacuation time of the first 40 pedestrians.

Table 2 shows the average evacuation time and standard deviation of the first 40 pedestrians in all experiments. We find that the NO case has the shortest average evacuation time of 19.225s. Both the CO and PO obstacle may worsen the evacuation efficiency. This is contrary to the findings of Helbing *et al* [5] and Yanagisawa *et al* [18], but consistent with previous studies [19], in which unreasonable obstacle location will increase evacuation time. The CO evacuation costs 32.7% extra time at a maximum. However, the difference in evacuation times between CO and PO is not evident. Some layouts of CO perform better than that of PO but some are worse. Note that, as the virtual room is made of tables and chairs in our experiment, the participants could

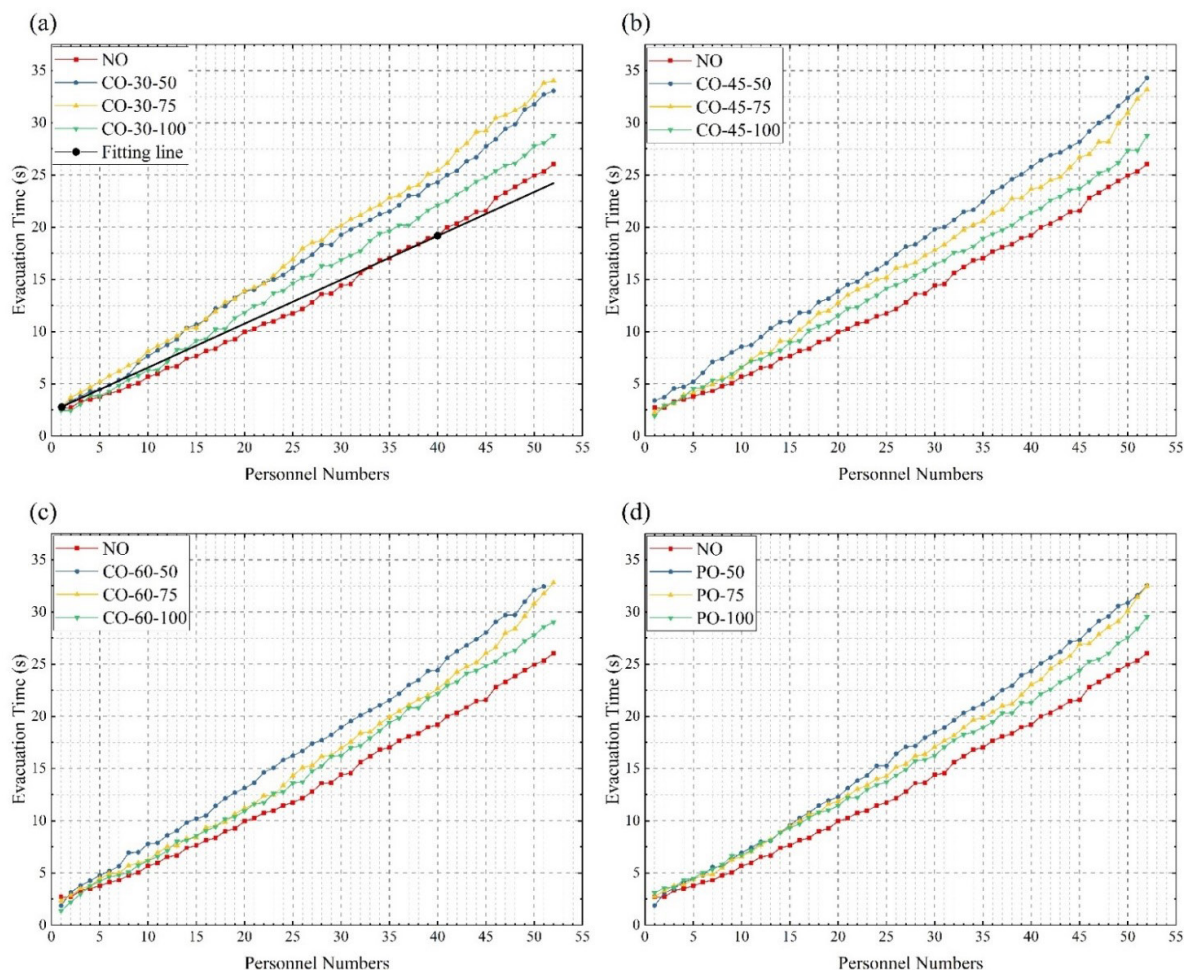


**Figure 2.** Evacuation time for each pedestrian in all sets of experiments. (a) NO and CO  $h = 30$  cm, (b) NO and CO  $h = 45$  cm, (c) NO and CO  $h = 60$  cm, (d) NO and PO. In (a), the fitting line is  $g_{40}$ .

obtain more global information. Therefore, they may choose a better path to avoid congestion. Also, participants can hang over the table at the exit area, which means more pedestrians may walk through the exit section at the same time. Both reasons will lead to higher outflow capacity than previous studies [28–30]. Generally speaking, the qualitative tendency is similar to previous studies. But our purpose is to investigate evacuation efficiencies. The exit made by tables is the same for NO, CO and PO settings. We can compare the evacuation difference between different obstacle settings qualitatively.

The  $p$  values from analysis of variance (ANOVA) for evacuation times in all sets of experiments are also given in table 3. ANOVA is a collection of statistical models and their associated estimation procedures (such as the ‘variation’ among and between groups) used to analyze the differences among group means in a sample. From tables 2 and 3 we can see that, on the whole, the evacuation time decreases with the increase in distance between the center of the obstacle and the exit. In terms of statistical results, most  $p$  values of ANOVA for evacuation time is smaller than 0.05, which means the difference in evacuation time under different experimental settings is significant. As shown in table 3, almost all the  $p$  values between NO time and others are 0.000.

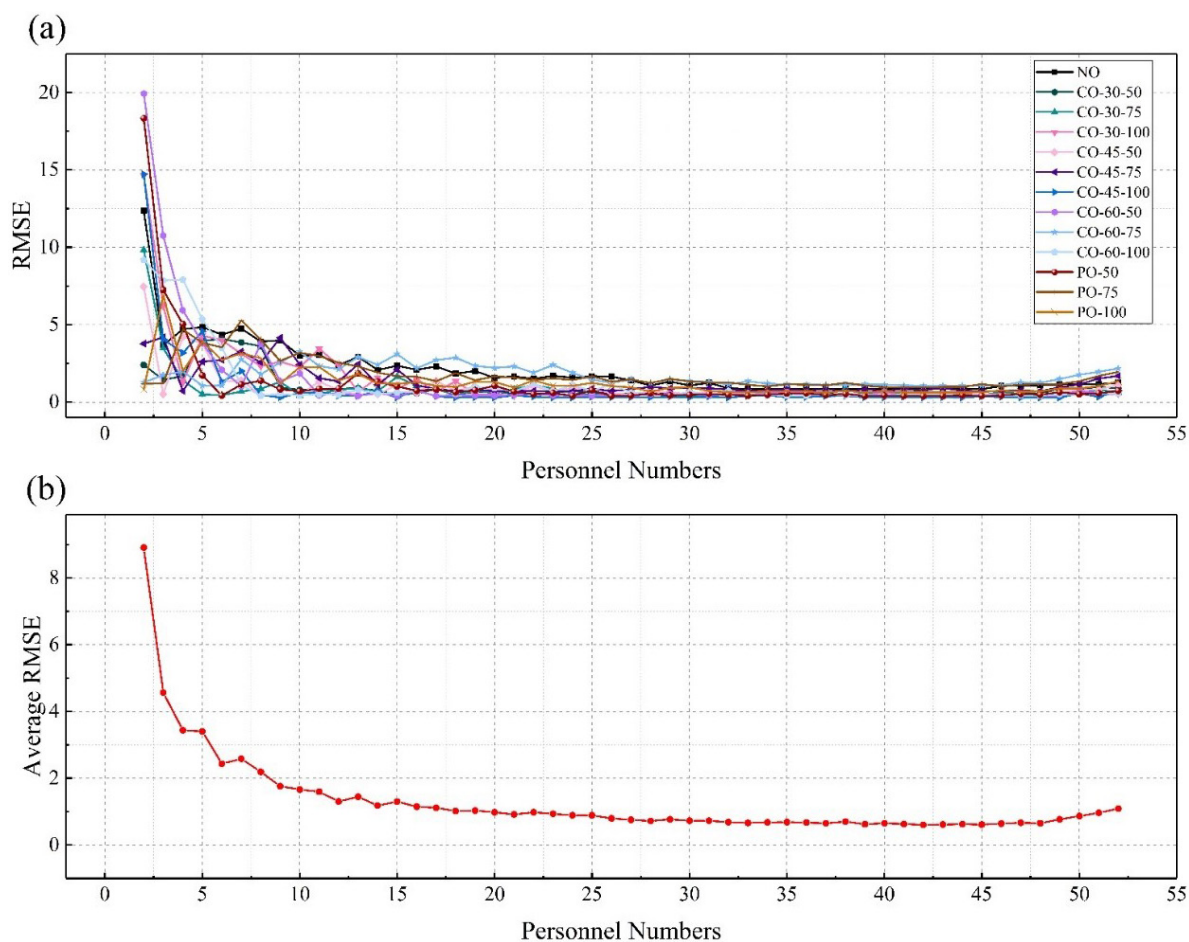


**Figure 3.** (a)  $RMSE(i)$  in each experiment (b) average RMSE in all experiments.

**Table 2.** Evacuation times in all sets of experiments.

Sequence number	Average time(s)	Standard deviation
NO	19.225	0.739
PO-100	20.891	0.728
CO-60-100	22.235	0.351
CO-45-100	22.228	0.851
CO-30-100	22.155	0.062
CO-30-50	23.597	0.735
CO-45-50	25.800	0.350
CO-60-50	24.718	0.639
PO-50	24.750	0.441
CO-30-75	24.834	0.725
CO-45-75	23.939	1.038
CO-60-75	23.462	0.733
PO-75	24.077	0.896

Therefore, the NO time is significantly shorter than all other cases. In the  $d = 100$  cm cases, the CO time is significantly larger than the PO time. Specifically, as  $h$  increases, the  $p$  values between CO time and PO time is 0.38, 0.29 and 0.28. Then, we compare the CO and PO times under the same  $d$ . When  $d$  is small (0.5, 0.75), on account of the

**Table 3.** *p* values of ANOVA for evacuation times in all sets of experiments.

	NO	CO-30-50	CO-30-75	CO-30-100	CO-45-50	CO-45-75	CO-45-100	CO-60-50	CO-60-75	CO-60-100	PO-50	PO-75	PO-100
NO	-	.000	.000	.000	.000	.000	.000	.000	.000	.000	.000	.000	.008
CO-30-50	.000	—	.042	.020	.001	<b>.560<sup>a</sup></b>	.026	<b>.064<sup>a</sup></b>	<b>.818<sup>a</sup></b>	.027	<b>.057<sup>a</sup></b>	<b>.414<sup>a</sup></b>	.000
CO-30-75	.000	.042	—	.000	<b>.107<sup>a</sup></b>	<b>.135<sup>a</sup></b>	.000	<b>.843<sup>a</sup></b>	.026	.000	<b>.887<sup>a</sup></b>	<b>.203<sup>a</sup></b>	.000
CO-30-100	.000	.020	.000	—	.000	.005	<b>.900<sup>a</sup></b>	.000	.033	<b>.891<sup>a</sup></b>	.000	.003	.038
CO-45-50	.000	.001	<b>.107<sup>a</sup></b>	.000	—	.003	.000	<b>.073<sup>a</sup></b>	.000	.000	<b>.081<sup>a</sup></b>	.006	.000
CO-45-75	.000	<b>.560<sup>a</sup></b>	<b>.135<sup>a</sup></b>	.005	.003	—	.007	<b>.190<sup>a</sup></b>	<b>.417<sup>a</sup></b>	.007	<b>.173<sup>a</sup></b>	<b>.813<sup>a</sup></b>	.000
CO-45-100	.000	.026	.000	<b>.900<sup>a</sup></b>	.000	.007	—	.000	.043	<b>.990<sup>a</sup></b>	.000	.004	.029
CO-60-50	.000	<b>.064<sup>a</sup></b>	<b>.843<sup>a</sup></b>	.000	<b>.073<sup>a</sup></b>	<b>.190<sup>a</sup></b>	.000	—	.039	.000	<b>.956<sup>a</sup></b>	<b>.279<sup>a</sup></b>	.000
CO-60-75	.000	<b>.818<sup>a</sup></b>	.026	.033	.000	<b>.417<sup>a</sup></b>	.043	.039	—	.044	.035	<b>.298<sup>a</sup></b>	.000
CO-60-100	.000	.027	.000	<b>.891<sup>a</sup></b>	.000	.007	<b>.990<sup>a</sup></b>	.000	.044	—	.000	.004	.028
PO-50	.000	<b>.057<sup>a</sup></b>	<b>.887<sup>a</sup></b>	.000	<b>.081<sup>a</sup></b>	<b>.173<sup>a</sup></b>	.000	<b>.956<sup>a</sup></b>	.035	.000	—	<b>.256<sup>a</sup></b>	.000
PO-75	.000	<b>.414<sup>a</sup></b>	<b>.203<sup>a</sup></b>	.003	.006	<b>.813<sup>a</sup></b>	.004	<b>.279<sup>a</sup></b>	<b>.298<sup>a</sup></b>	.004	.256	—	.000
PO-100	.008	.000	.000	.038	.000	.000	.029	.000	.000	.028	.000	.000	—

<sup>a</sup> *p* ≥ 0.05.

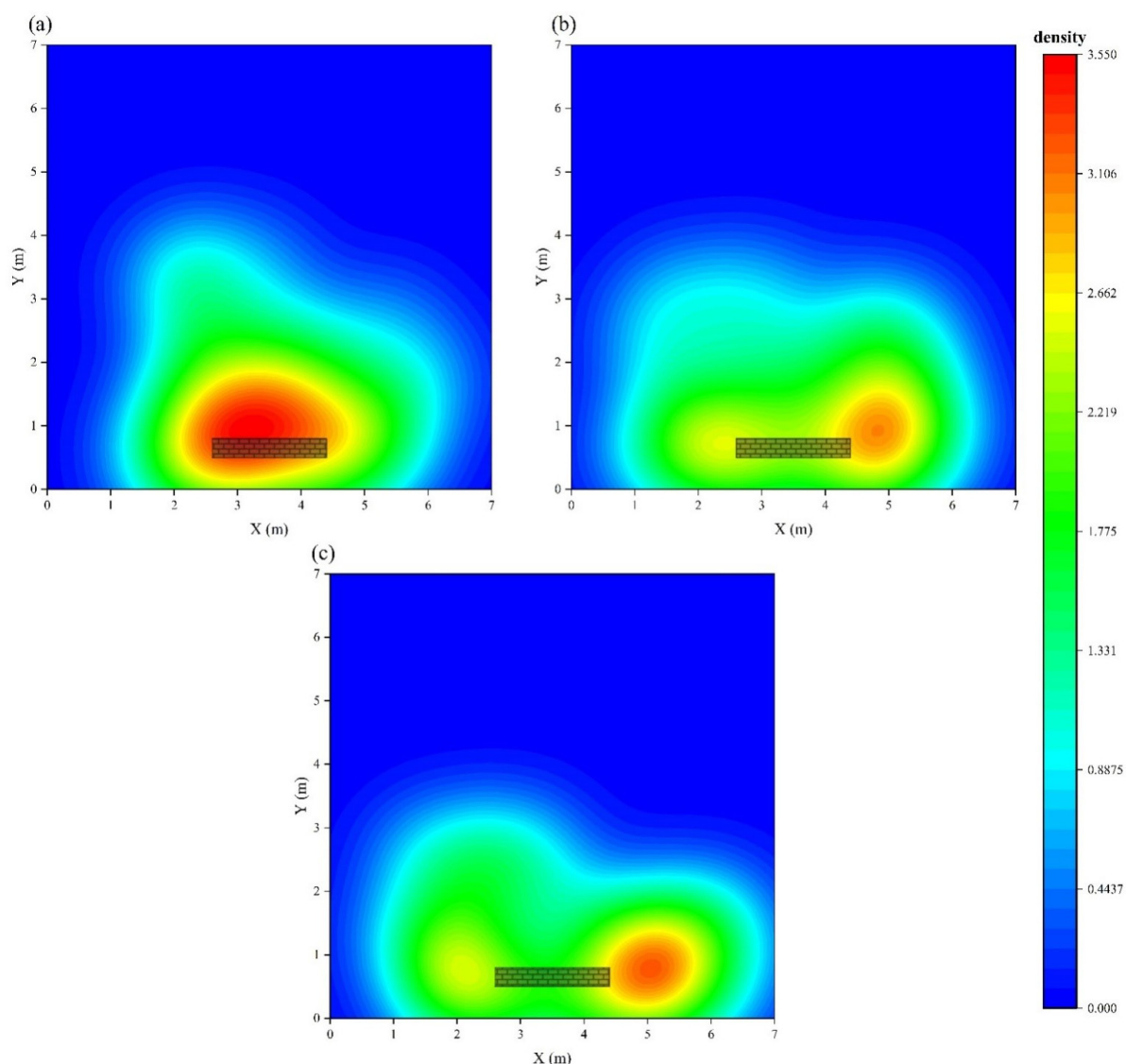


**Figure 4.** Density distribution in  $d = 50$  cm CO experiments at  $t = 10$  s. (a)  $h = 30$  cm, (b)  $h = 45$  cm, (c)  $h = 60$  cm.

congestion, there are still many pedestrians who choose to bypass the obstacle instead of stepping over it, and it also means the CO cases have no significant difference to the PO cases. For example, in the  $d = 50$  cm cases, all the  $p$  values between PO time and CO time are larger than 0.05, especially in the  $h = 60$  cm CO case, where the value reaches 0.956. Note that in the  $d = 50$  cm CO cases, with the increase in obstacle height, the evacuation time increases at first and then decreases. Also, in the  $h = 30$  cm CO cases, as the distance between the obstacle and the exit increases, the evacuation time also grows at first and then decreases. However, when  $d = 100$  cm, the CO time and PO time show a significant difference ( $p < 0.05$ ). It is plausible that this is due to the experiments with 100 cm distance between the obstacle and the exit are conducted first. Thus participants take more time to adapt to the CO conditions. In addition, in the  $d = 100$  cm cases, congestion has little impact on the pedestrians' choice of stepping over the obstacle and more pedestrians choose to step over the obstacle due to curiosity. At

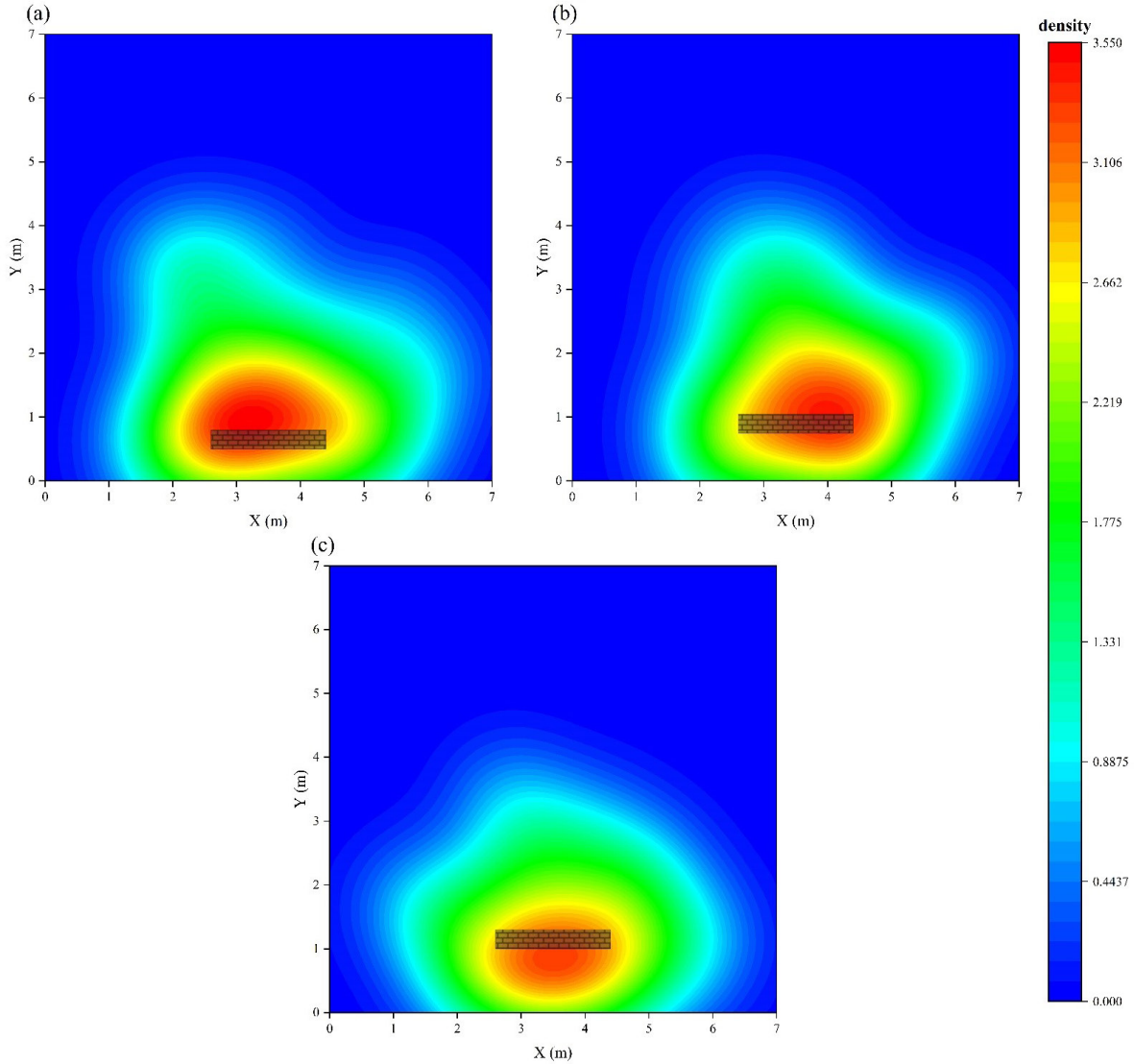


**Figure 5.** Density distribution in  $h = 30$  cm CO experiments at  $t = 10$  s. (a)  $d = 50$  cm, (b)  $d = 75$  cm, (c)  $d = 100$  cm.

last, we compare the CO times with the same obstacle height. From table 3, any two CO times with the same  $h$  but different  $d$  have a significant difference ( $p < 0.05$ ). This means that the distance between the small obstacle and the exit has an indispensable effect on the evacuation time.

To discover the reason for nonmonotonicity in the evacuation time and the influence of obstacles on pedestrian evacuation dynamics, local density distribution is studied. The local density is calculated in the same way as Helbing *et al* [31] calculated it:

$$\rho(\vec{r}, t) = \sum_j f(\vec{r}_j(t) - \vec{r}). \tag{2}$$

Here  $\vec{r}_j(t)$  is the position of the  $j$ th pedestrian which is in the vicinity of  $\vec{r}$  and

$$f(\vec{r}_j(t) - \vec{r}) = \frac{1}{\pi R^2} \exp\left[-\|\vec{r}_j(t) - \vec{r}\|^2 / R^2\right] \tag{3}$$

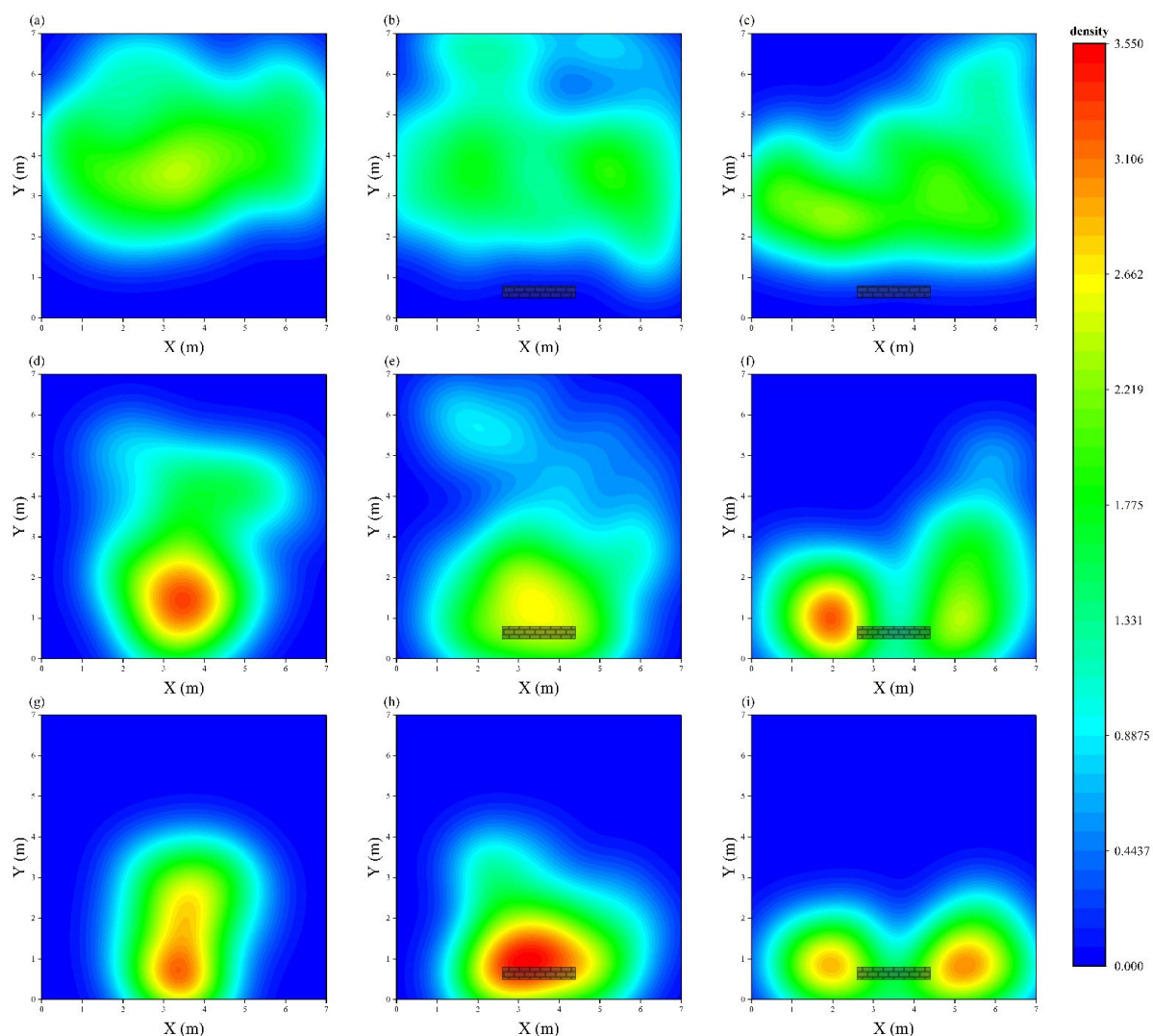


**Figure 6.** Contour plots of local density. Left: NO experiment; middle: CO experiment,  $d = 50$  cm,  $h = 30$  cm; right: PO experiment,  $d = 50$  cm. (a)–(c)  $t = 0$  s; (d)–(f)  $t = 5$  s; (g)–(i)  $t = 10$  s. The horizontal and vertical coordinates represent the corresponding coordinate values of pedestrians in the room.

is a distance-dependent Gaussian weight function.  $R$  is a measurement parameter. The greater  $R$  is, the greater the effective measurement radius is. We set  $R = 1$  m in this paper as did Helbing *et al* [31]. Although the Voronoi diagram of the XT method seems a little more accurate, what concerns us is the qualitative changes of density caused by different experimental conditions. By using Helbing *et al*'s [31] method, the local density becomes smoother in the whole area. So it is a better way to show the tendency in the experimental room.

Figure 4 shows the density distribution in  $d = 50$  cm of CO cases at  $t = 10$  s. When the obstacle height is 30 cm, pedestrians prefer to step over the obstacle. The obstacle height has relatively little effect on pedestrian movement. So there is only one high-density cluster near the exit. With the obstacle height increased to 45 cm, more pedestrians choose to pass by the obstacle, and the high-density area separates into two clusters around the obstacle. At an obstacle height  $h = 60$  cm, few pedestrians step over

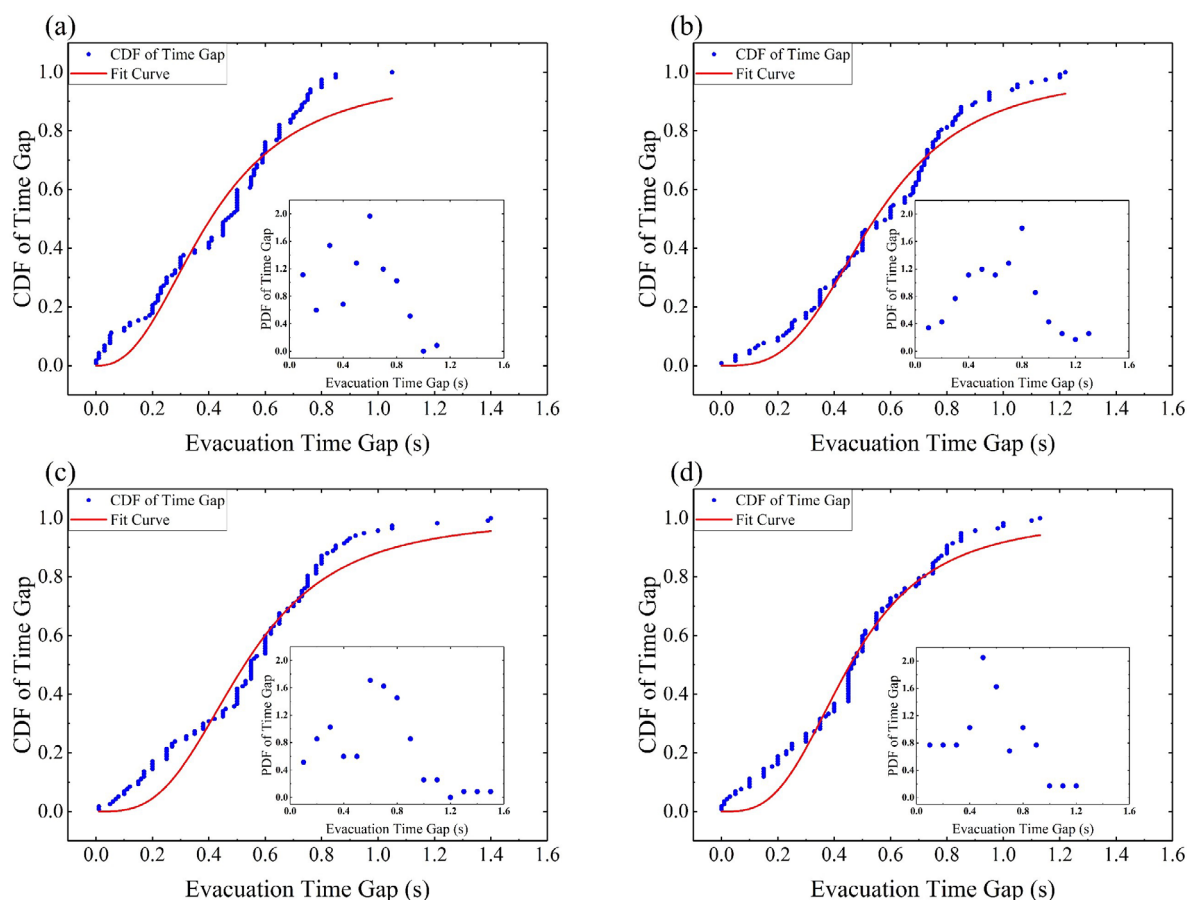


**Figure 7.** Cumulative density distribution function and its fitting curve of evacuation time gaps in NO and PO experiments. (a) NO experiment. (b) PO experiment,  $d = 50$  cm. (c) PO experiment,  $d = 75$  cm. (d) PO experiment,  $d = 100$  cm. The logistic distribution is used as the fitting curve. Inset: the probability density distribution.

the obstacle. Only with  $h = 45$  cm does there exist more interactions between pedestrians bypassing the obstacle and those stepping over it, resulting in a longer evacuation time. Therefore, although the obstacle height has a trivial effect on evacuation time, it determines the different density distributions.

Figure 5 shows the density distribution in  $h = 30$  cm of CO cases at  $t = 10$  s. When the distance between the obstacle and the exit is 50 cm, the center of the high-density cluster is behind the obstacle (1 m away from the exit). The pedestrians have a small space to adjust their steps to step over the obstacle. With the movement of the obstacle to 75 cm, the cluster center (1 m away from the exit) is located nearly on the obstacle. The pedestrians have to struggle in one small space to manage the interaction with the obstacle at first, which costs extra time. Then as the obstacle moves to 100 cm, the cluster center (0.75 m away from the exit) is located between the obstacle and the exit. The obstacle has a much smaller effect on the cluster dynamics.

Comparing with  $d = 50$  cm CO cases, there is more space between obstacle and exit in  $d = 75$  cm CO cases. More pedestrians can choose to pass by the obstacle to escape the room. So no nonmonotonicity is found in  $d = 75$  cm CO cases. Although

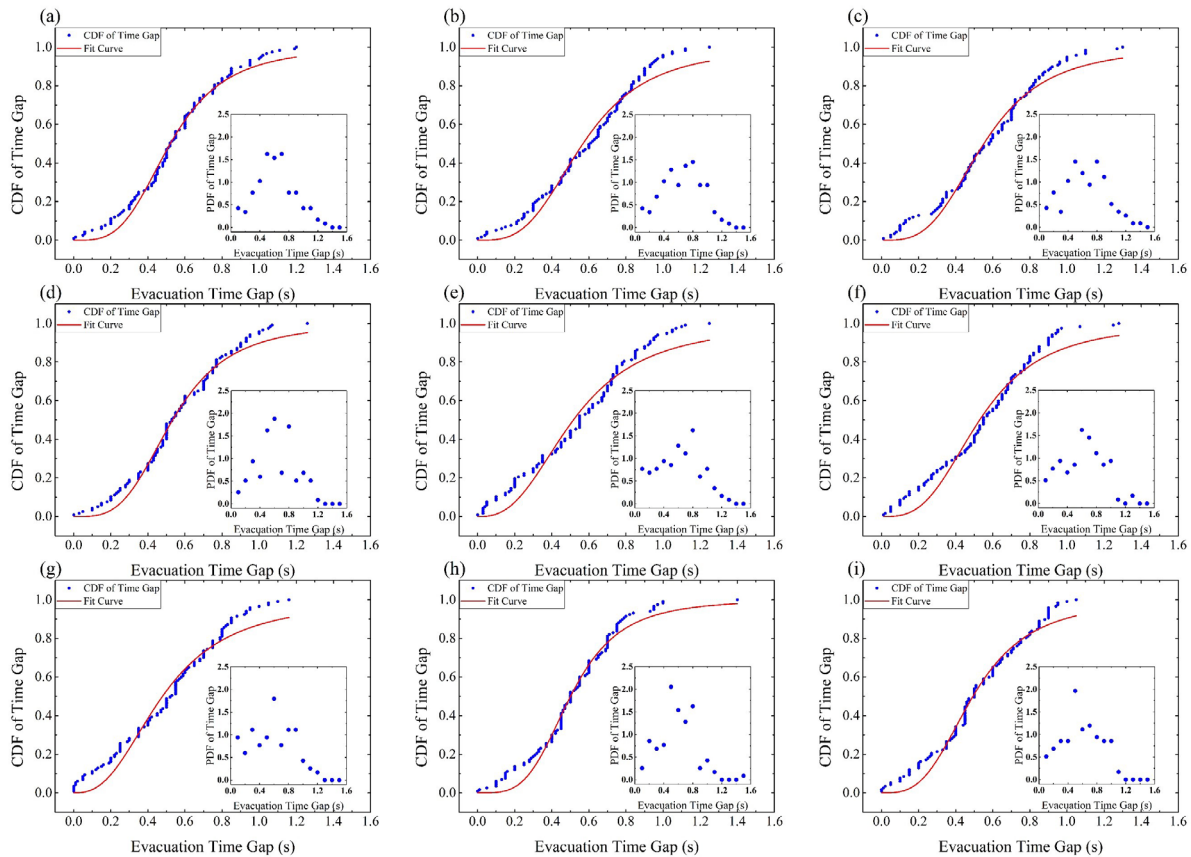


**Figure 8.** Cumulative density distribution function and its fitting curve of evacuation time gaps in CO experiments. (a)  $h = 30$  cm,  $d = 50$  cm. (b)  $h = 45$  cm,  $d = 50$  cm. (c)  $h = 60$  cm,  $d = 50$  cm. (d)  $h = 30$  cm,  $d = 75$  cm. (e)  $h = 45$  cm,  $d = 75$  cm. (f)  $h = 60$  cm,  $d = 75$  cm. (g)  $h = 30$  cm,  $d = 100$  cm. (h)  $h = 45$  cm,  $d = 100$  cm. (i)  $h = 60$  cm,  $d = 100$  cm. The logistic distribution is used as the fitting curve. Inset: the probability density distribution.

nonmonotonicity is shown in our laboratory experiments, the small sample size and randomness may be an alternative reason for the phenomenon, and we will do more work to verify the correctness of these results.

### 3.2. Density evolution

Figure 6 shows the typical local density distribution at different times. At the initial time, all pedestrians stand behind the waiting line. The distributions are relatively uniform, and there is no significant difference in NO, CO and PO experiments (figures 6(a)–(c)). After the experiment starts (figures 6(d)–(f)), pedestrians walk to the exit. In the NO case, pedestrians congest behind the exit. No obvious jam forms around the obstacle at the fifth second after the beginning in the CO case. In contrast, a pedestrian cluster emerges around the obstacle corner in the PO case. As the experiment goes on, the high density areas in the NO and PO cases remain unchanged (figures 6(g) and (i)). However, the congestion in the CO case becomes more serious, and the highest density is even larger than that in the NO or PO cases.

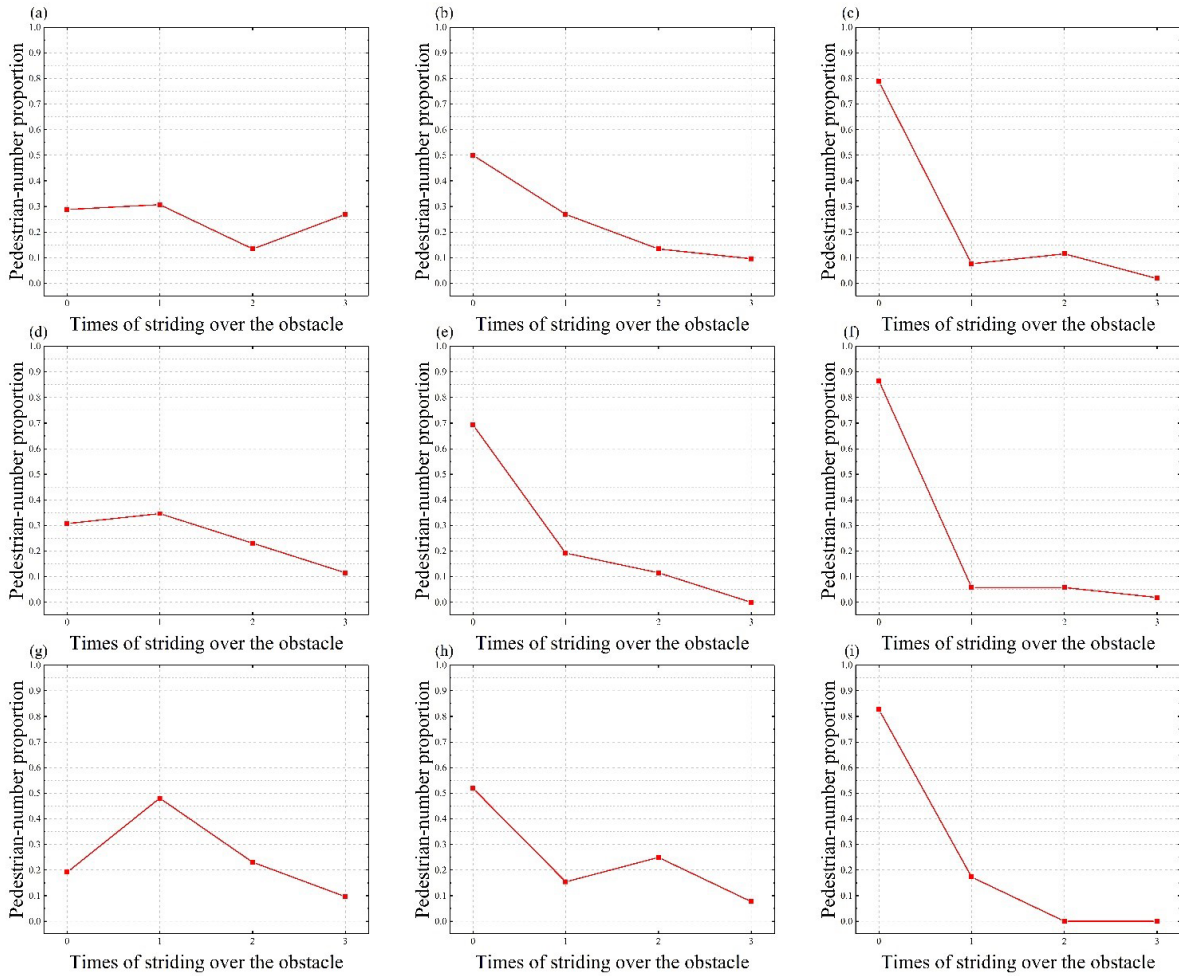


**Figure 9.** The pedestrian-number proportion against stepping over times of one pedestrian in three repetitions. (a)  $h = 30$  cm,  $d = 50$  cm. (b)  $h = 45$  cm,  $d = 50$  cm. (c)  $h = 60$  cm,  $d = 50$  cm. (d)  $h = 30$  cm,  $d = 75$  cm. (e)  $h = 45$  cm,  $d = 75$  cm. (f)  $h = 60$  cm,  $d = 75$  cm. (g)  $h = 30$  cm,  $d = 100$  cm. (h)  $h = 45$  cm,  $d = 100$  cm. (i)  $h = 60$  cm,  $d = 100$  cm.

### 3.3. Evacuation time gap

The evacuation time gap  $\Delta t$  is used to describe the time difference between consecutive pedestrians, which is calculated as follows

$$\Delta t_i = t_{i+1} - t_i. \tag{4}$$

Here,  $t_{i+1}(t_i)$  is the time  $i + 1$ th ( $i$ th) pedestrian escapes from the room in chronological order.

We calculated the cumulative density distribution of evacuation time gaps for all experiments. Logistic distribution is used to fit them, as seen in figures 7 and 8. As we can see, the cumulative distribution of evacuation time gaps in our experiments is fitted pretty well by logistic distribution. From table 4, we can see that all the  $R$ -square values are greater than 0.9, meaning that logistic distribution can match the experimental result very well. It can be seen that the cumulative density distribution function rose

**Table 4.** Fitting parameters of fitting curve of cumulative density distribution function of evacuation time gaps in all experiments.

	$x_0$		$p$		Statistics	
	Value	Std. error	Value	Std. error	Reduced chi-square	Adj. $R$ -square
NO	0.4061	0.00607	2.44471	0.09636	0.0046	0.94532
PO-50	0.54446	0.00409	3.15	0.08099	0.00206	0.97548
PO-75	0.52661	0.00582	3.14561	0.13039	0.00408	0.95142
PO-100	0.45606	0.00418	3.07741	0.10478	0.00285	0.96607
CO-30-50	0.52045	0.00261	3.48418	0.07128	0.00115	0.98628
CO-45-50	0.56784	0.00446	3.2296	0.08904	0.00233	0.97232
CO-60-50	0.5514	0.00377	3.27365	0.08146	0.00183	0.9782
CO-30-75	0.53323	0.00288	3.4598	0.07351	0.00131	0.98438
CO-45-75	0.51616	0.00639	2.65829	0.09839	0.00372	0.95571
CO-60-75	0.529	0.0055	3.06606	0.11213	0.00349	0.95846
CO-30-100	0.47862	0.00579	2.58698	0.09039	0.00339	0.95963
CO-45-100	0.50094	0.0029	3.76753	0.09576	0.00176	0.97904
CO-60-100	0.49291	0.00363	3.17479	0.08516	0.00202	0.97598

Logistic distribution:  $y = 1 - 1/(1 + (x/x_0)^p)$

fastest in the interval [0.4, 0.8 s], which means most evacuation time gaps are concentrated in this interval, i.e. the range of high PDF values in the insets.

Specifically, from the probability density distribution, with the distance between the obstacle and the exit increasing in the PO cases, the peak time gap distribution moves from 0.7–0.8 s to about 0.4–0.5 s, which is almost the same as that in the NO case (figure 7(a)). The peaks of time gap distribution in the CO cases (figure 8) are universally larger than those in the NO and PO cases. Generally speaking, a long evacuation time will lead to a relatively large time gap. Also, the peaks of the fitting lines are almost all around 0.5 s, which are a little larger than in previous studies [8]. The reason is that the experiments are conducted under normal conditions without any panic, so pedestrians remain in a bigger personal space away from others. Some experimental results did not fit well, which may be due to the small sample size and randomness.

### 3.4. Step over or bypass the obstacle

We have carried out the CO experiment a total of 27 times repeatedly to test whether pedestrians will step over or bypass the obstacles when facing obstacles of different heights. We obtained the data from one pedestrian as the bypassing individual or over-stepping individual in one of the experiments. The total number of pedestrians choosing to step over the obstacle in each case is analyzed. To explore the collective behavior of pedestrians in the CO cases, the proportion of evacuees with different stepping over times (of one pedestrian) in each set of three experiments (repeated three times) are shown in figure 9. As the distance between obstacle and exit increases, more pedestrians choose to pass by the obstacle. Fewer pedestrians prefer to step over repeatedly. The possible reason may be that in the  $d = 50$  cm case, the space between obstacle and exit is limited, so pedestrians have to step over the obstacle to get out of the room sooner. As the height of the obstacle increases, the number of over-stepping pedestrians decreases.

## 4. Conclusions

In this study, we investigate evacuation dynamics through a series of well-controlled experiments. 52 participants took part in 13 sets of experiments, including evacuation without obstacle (NO), evacuation with an obstacle that can be stepped over or passed by (CO), and evacuation with an obstacle that can only be passed by (PO). It is observed that evacuation time shows a nearly linear relationship with the pedestrian number escaping from the room. Evacuation in the NO case has the shortest average evacuation time. In the CO and PO cases, the evacuation time decreases along with the increase in distance between obstacle and exit. Furthermore, the longer the distance between obstacle and exit, the better the PO obstacle performed. However, when the CO obstacle is too close to the exit and its height is very low, it can help to reduce evacuation time compared to the PO obstacle. In particular, the impact of the CO obstacle on evacuation time is not monotonous. Its height will lead to different cluster distributions, and its distance from the exit will affect the pace adjustment of pedestrians in the cluster. Moreover, as the distance between obstacle and exit increases, more pedestrians prefer to pass by the CO obstacle. The lesson we can learn is that a small obstacle near the exit will decrease evacuation efficiency. It is better to situate small objects (such as chairs, tea counter, shelves and so on) far away from the room door. There is no denying that these are just the results of laboratory experiments using young educated participants, and we will do more work to verify the correctness of these results. In the future, more experiments should be conducted to study the effect of the different shapes of CO obstacles on pedestrian dynamics, such as balls, cylinders and irregular shapes. Also, the result should be checked in a real room.

## Acknowledgments

This work is supported by the National Key Research and Development Program of China (Grant No. 2018YFB1600900), the National Natural Science Foundation of China (Grants Nos. 71671058, 71704046, 71801066), Anhui Provincial Natural Science Foundation (Grant No. 1808085QG225), and the Fundamental Research Funds for the Central Universities (Grant No. PA2019GDQT0020).

## References

- [1] Henderson L F 1971 The statistics of crowd fluids *Nature* **229** 381–3
- [2] Fruin J J 1971 Designing for Pedestrians: A Level of Service Concept *Highway Research Record* **355** 1–15
- [3] Mawson A R 2007 *Mass Panic and Social Attachment: The Dynamics of Human Behavior* (Farnham: Ashgate)
- [4] Helbing D, Farkas I and Vicsek T 2000 Simulating dynamical features of escape panic *Nature* **407** 487–90
- [5] Helbing D, Buzna L, Johansson A and Werner T 2005 Self-organized pedestrian crowd dynamics: experiments, simulations, and design solutions *Transp. Sci.* **39** 1–24
- [6] Shiwakoti N, Sarvi M, Rose G and Burd M 2011 Animal dynamics based approach for modeling pedestrian crowd egress under panic conditions *Transp. Res. B* **45** 1433–49
- [7] Jiang L, Li J, Shen C, Yang S and Han Z 2014 Obstacle optimization for panic flow—reducing the tangential momentum increases the escape speed *PLoS One* **9** 12
- [8] Guo N, Jiang R, Hu M-B and Ding J-X 2017 Constant evacuation time gap: experimental study and modeling *Chin. Phys. B* **26** 120506

- [9] Shi X, Ye Z, Shiwakoti N and Grembek O 2018 A state-of-the-art review on empirical data collection for external governed pedestrians complex movement *J. Adv. Transp.* **1**–42
- [10] Muramatsu M, Irie T and Nagatani T 1999 Jamming transition in pedestrian counter flow *Physica A* **267** 487–98
- [11] Zahra Shahhoseini M S 2019 Pedestrian crowd flows in shared spaces: investigating the impact of geometry based on micro and macro scale measures *Transp. Res. B* **122** 57–87
- [12] Fu Z *et al* 2015 A floor field cellular automaton for crowd evacuation considering different walking abilities *Physica A* **420** 294–303
- [13] Zhou X, Hu J, Ji X and Xiao X 2019 Cellular automaton simulation of pedestrian flow considering vision and multi-velocity *Physica A* **514** 982–92
- [14] Isobe M, Helbing D and Nagatani T 2004 Experiment, theory, and simulation of the evacuation of a room without visibility *Phys. Rev. E* **69** 066132
- [15] Nagai R, Nagatani T, Isobe M and Adachi T 2004 Effect of exit configuration on evacuation of a room without visibility *Physica A* **343** 712–24
- [16] Guo R-Y, Huang H-J and Wong S C 2012 Route choice in pedestrian evacuation under conditions of good and zero visibility: experimental and simulation results *Transp. Res. B* **46** 669–86
- [17] Wang P and Cao S 2019 Simulation of pedestrian evacuation strategies under limited visibility *Phys. Lett. A* **383** 825–32
- [18] Yanagisawa D *et al* 2009 Analysis on pedestrian outflow through an exit with an obstacle *ICCAS-SICE* 5040–5045
- [19] Yiwen L, Xiaomeng S, Zhirui Y, Shiwakoti N and Junkai L 2016 Controlled experiments to examine different exit designs on crowd evacuation dynamics *CICTP 2016* pp 779–90
- [20] Shi X, Ye Z, Shiwakoti N, Tang D and Lin J 2018 Examining effect of architectural adjustment on pedestrian crowd flow at bottleneck *Physica A* **522** 350–64
- [21] Garcimartin A, Maza D, Pastor J M, Parisi D R, Martin-Gomez C and Zuriguel I 2018 Redefining the role of obstacles in pedestrian evacuation *New J. Phys.* **20** 8
- [22] Shiwakoti N, Shi X and Ye Z 2019 A review on the performance of an obstacle near an exit on pedestrian crowd evacuation *Saf. Sci.* **113** 54–67
- [23] Lu X Z, Yang Z B, Cimellaro G P and Xu Z 2019 Pedestrian evacuation simulation under the scenario with earthquake-induced falling debris *Saf. Sci.* **114** 61–71
- [24] Delcea C, Cotfas L-A, Craciun L and Molanescu A G 2020 An agent-based modeling approach to collaborative classrooms evacuation process *Saf. Sci.* **121** 414–29
- [25] Zhao Y *et al* 2017 Optimal layout design of obstacles for panic evacuation using differential evolution *Physica A* **465** 175–94
- [26] Zhang J, Song W G and Xu X 2008 Experiment and multi-grid modeling of evacuation from a classroom *Physica A* **387** 5901–9
- [27] von Kruchten C and Schadschneider A 2017 Empirical study on social groups in pedestrian evacuation dynamics *Physica A* **475** 129–41
- [28] Daamen W and Hoogendoorn S 2010 *Capacity of Doors during Evacuation Conditions* ed S P Hoogendoorn *et al (1st Conf. on Evacuation Modeling and Management)* (Amsterdam: Elsevier) pp 53–66
- [29] Bode N W F, Holl S, Mehner W and Seyfried A 2015 Disentangling the impact of social groups on response times and movement dynamics in evacuations *PLoS One* **10** 14
- [30] Haghani M and Sarvi M 2019 Simulating pedestrian flow through narrow exits *Phys. Lett. A* **383** 110–20
- [31] Helbing D, Johansson A and Al-Abideen H Z 2007 Dynamics of crowd disasters: an empirical study *Phys. Rev. E* **75** 046109